Studies of Pyridinyl-Containing 14-Membered Macrocyclic Copper(II) Complexes

Sabrina Autzen,[a] Hans-Gert Korth,[a] Roland Boese,[b] Herbert de Groot,*[c] and Reiner Sustmann*[a]

Keywords: Macrocyclic ligands / Copper / Enzyme models / Superoxide dismutase

Six copper(II) complexes of tetracoordinating, pyridinyl-containing 14-membered macrocycles with varying ratios of nitrogen and oxygen donor atoms were prepared and characterized by IR, UV/Vis, and EPR spectroscopy and cyclic voltammetry. A distorted tetragonal coordination of the copper center in the solid-state was established by X-ray crystallography for the tetraazamacrocyclic complex **Cu-3** carrying a methoxybenzyl pendent arm and the trioxaaza complex **Cu-6**. The superoxide dismutase-like activity of the Cu^{II} complexes was investigated by inhibition of NADH oxidation. Although the UV/Vis and EPR spectra of the complexes were strongly affected when the coordinating nitrogen atoms were successively replaced by oxygen atoms, no significant change in their reactivity towards superoxide was observed. In all cases a 1:1 or 1:2 stoichiometry for the reaction with superoxide was found, with the exception of the methoxybenzyl-substituted tetraaza complex, which showed a low catalytic activity with a turnover number of about 10.

Introduction

Our present studies are concerned with the preparation of transition metal complexes of 14-membered, pyridine-containing macrocycles and the examination of their spectroscopic properties to elucidate their potential enzyme-mimetic qualities. We have recently reported the catalase-mimetic activity of some non-heme iron(III) complexes.[1] Copper is another biologically significant metal, being found in various enzymes, such as the important Cu-Zn superoxide dismutase (Cu_2Zn_2-SOD), which is used in living organisms to detoxify the superoxide radical anion, $O_2^{\cdot -}$, [Equation (1)].[2]

$$2\,O_2^{\cdot -} + 2\,H^+ \xrightarrow{SOD} H_2O_2 + O_2 \qquad (1)$$

[a] Institut für Organische Chemie, Universität Essen, Universitätsstr. 5, 45117 Essen, Germany
Fax: (internat.) + 49-201/183-4259
E-mail: reiner.sustmann@uni-essen.de
[b] Institut für Anorganische Chemie, Universität Essen, Universitätsstr. 5, 45117 Essen, Germany
[c] Institut für Physiologische Chemie, Universitätsklinikum Essen, Hufelandstr. 55, 45122 Essen, Germany
Fax: (internat.) + 49-201/723-5943
E-mail: h.de.groot@uni-essen.de

Numerous transition metal (preferably Cu, Fe, Mn) complexes of various kinds have been investigated with regard to their reactivity toward superoxide. The use of copper complexes as SOD mimics has been reviewed.[3,4] Although several investigated compounds exhibit good SOD-like activities, systematic studies concerning the factors which govern the enzyme-mimicking reactivities are scarce.[5] We report here on the copper(II) complexes **Cu-1**−**Cu-6** of ligands **1**−**6** in which the sp^3-nitrogen atoms of the parent macrocycle **1** are successively replaced by oxygen atoms. Spectroscopic properties were compared to determine the influence of the coordinating atoms on the SOD-like activities of the complexes. Complexes **Cu-1** and **Cu-2** have previously been described,[6−9] but their SOD activity was not investigated. Complex **Cu-3**, carrying a methoxybenzyl pendent arm, was included in this study to determine whether a possible coordination by the phenolic oxygen atom to the fifth coordination site at the copper atom might influence the catalytic activity. Coordination of phenolate groups to the fifth position in square-planar Cu^{II} complexes has been reported before;[10] however, to the best of our knowledge, coordination of phenyl ether substituents to the axial position has not been reported. There is, however, a recent report[11] in which phenyl ether moieties within the chain of a 20-membered macrocyclic ligand bind to the axial position of a tetra-*N*-coordinated copper(II) complex. X-ray crystal structures of the copper(II) complexes **Cu-3** and **Cu-6** are presented. X-ray structures of eight 14-membered *endo*-pyridine Cu^{II} complexes, including the PF_6^- salt of

Cu-1,[9] can be found in the Cambridge Structural Database.[12]

Results and Discussion

Synthesis

Macrocycle **2** was prepared from its nickel complex as described by Karn and Busch.[13] Compound **5** was prepared from ditosylated pyridine-2,6-diyldimethanol and the alkanediol, compound **6**[14] from pyridine-2,6-diyldimethanol and the appropriate alkanediyl ditosylate. Macrocycles **1**[6] and **3**[1] were prepared according to literature procedures in a copper-template reaction. The preparation of ligands **1**, **3** and **4** was devised starting from pyridine-2,6-dicarbaldehyde, which was treated with the appropriate diamine in a copper-template reaction to give the macrocycle. Diimine reduction by sodium borohydride and removal of copper(II) as sulfide provided the free ligands. Unfortunately, attempts to prepare the macrocycles **7** and **8**, in which the position of the nitrogen and oxygen atoms was exchanged with respect to compounds **4** and **5**, respectively, were not successful (Scheme 1).

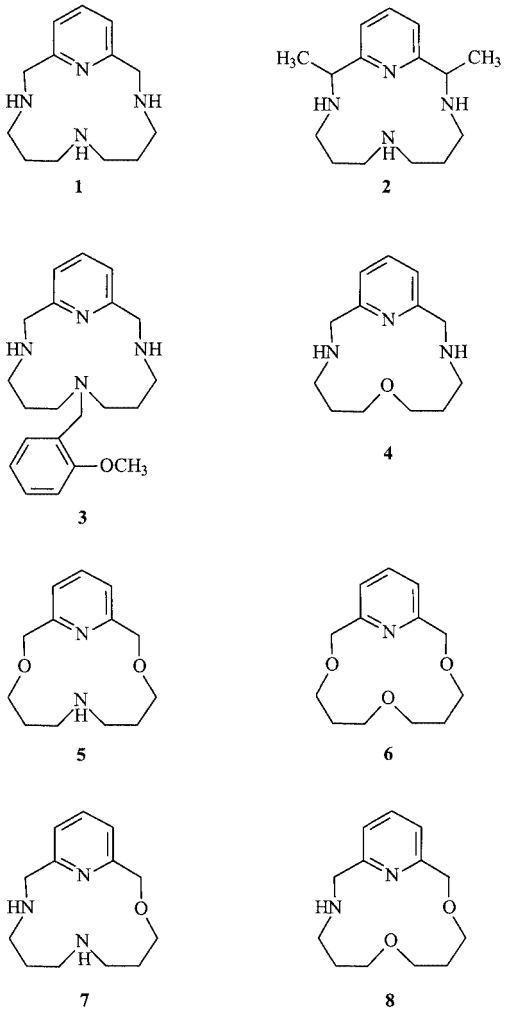

Scheme 1

Facile formation of the copper(II) complexes was achieved by addition of an equimolar ethanolic solution of copper(II) perchlorate to an ethanolic solution of the ligands at room temperature and subsequent crystallization. As expected, for the ligands **1**, **2**, and **4**−**6** the corresponding copper complexes **Cu-1**, **Cu-2**, and **Cu-4**−**Cu-6** (Scheme 2) with two perchlorate counterions were obtained.

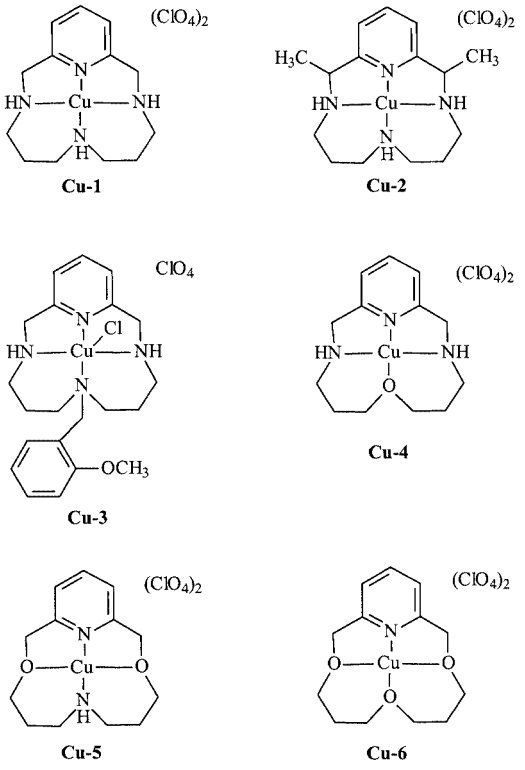

Scheme 2

Unexpectedly, X-ray structural and elemental analysis revealed that the copper complex **Cu-3** of ligand **3** contained one chloride ion as a counterion, although no chloride was involved in any steps of the synthesis. Thus, perchlorate must have been reduced during complex formation. Although perchlorate (which is a weakly chelating, relatively large anion) is a strong oxidant it is generally kinetically stable to reductants and is therefore frequently used to regulate the ion strength in kinetic and thermodynamic studies.[15] Because perchlorate reduction was not observed in the preparation of the related complexes **Cu-1** and **Cu-2**, it is very likely that the methoxybenzyl side chain of **3** facilitated this reduction. This conclusion is supported by the rapid formation of a Cu^{II}+**3** complex of 1:2 stoichiometry, $[Cu^{II}(\mathbf{3})_2](ClO_4)_2$, after mixing of copper(II) perchlorate and **3** (see Exp. Sect.). When kept in the reaction mixture, this complex slowly (within 12 h) converted into complex **Cu-3**. We propose that the initial 1:2 complex may have been formed by a kinetically controlled, exocyclic complexation, probably involving the oxygen atom of the methoxybenzyl

substituent. In solution, this exocyclic complex then rearranges to the thermodynamically more stable complex **Cu-3**, thereby re-releasing one ligand molecule. Concomitantly, partial reduction of perchlorate to chloride takes place. Given the rather mild reaction conditions used here it is not clear how the perchlorate might have been reduced, i.e. which chemical entity would have been the reductant. The copper(II) ion is unlikely to be oxidized under the applied conditions (compare the inertness of **Cu-1**, **Cu-2**), whereas the electron-rich phenyl group of the side arm might be a chemically reasonable target. A reduction of perchlorate to chloride during the preparation of a macrocyclic iron complex has been described by Goedken et al.[16] who discussed the formation of an unspecified, yet very reactive, intermediate. Elucidation of the mechanism of this interesting reaction is beyond the scope of this paper and will be the subject of a separate study.

Crystal Structure

The crystal structure of **Cu-1** with two PF_6^- counterions instead of perchlorate has been reported.[9] The crystal structures and the unit-cell diagrams of **Cu-3** and **Cu-6** are displayed in Figures 1 and 2. Selected bond lengths and angles are listed in the captions. It can be seen that in **Cu-3** copper(II) has a fivefold coordination environment. The four in-plane distances are of lengths commonly found in square-based pyramidal structures, with the $Cu-N_{pyr}$ distance (1.94 Å) being somewhat shorter than the other C−N distances (2.02−2.05 Å). This bond-length pattern seems to be characteristic of complexes of tetraazamacrocyclic ligands containing a pyridine moiety (see refs.[1,9] and references cited therein). The copper(II) ion in **Cu-3** is lifted out of the plane of the four coordinating ligand atoms by ρ(**Cu-3**) = 0.311 Å with a $Cu^{II}-Cl$ distance of 2.564 Å. The tetrahedral distortion of 0.311 Å is significantly increased compared with that in **Cu-1**·$(PF_6)_2$ (ρ = 0.133 Å),[9] which may be related to the coordination of Cl^-. The methoxybenzyl group, C(15)−C(21) and O(1), with the riding hydrogen atoms and the methylene hydrogen atoms H(14A/14B) is disordered over two sites with occupancies of 0.6 and 0.4 together; O(31) and C(32) of the methoxy group are disordered over two sites with occupancies of 0.5. In the crystal, the oxygen atom of the 2-methoxybenzyl group is not coordinated to the central ion. The second counterion is essentially noncoordinating perchlorate. Unlike **Cu-3**, in **Cu-6** the copper atom is essentially located in-plane [ρ(**Cu-6**) = 0.003 Å], with a Cu−N distance of 1.89 Å and Cu−O lengths of 1.93−1.96 Å. One of the perchlorate anions is

Table 1. Crystallographic data of **Cu-3** and **Cu-6**

Compound	**Cu-3**	**Cu-6**
Empirical formula	$C_{21}H_{30}ClCuN_4O\cdot ClO_4\cdot 0.5[CH_4O]$	$C_{13}H_{19}CuNO_3\cdot 2[ClO_4]$
Formula mass	568.95	499.73
Temperature [K]	203(2)	203(2)
Wavelength [Å]	0.71073	0.71073
Crystal system	triclinic	monoclinic
Space group	$P\bar{1}$	$P2_1$
a [Å]	6.8494(12)	9.739(2)
b [Å]	10.764(2)	7.1341(17)
c [Å]	17.819(3)	13.785(3)
α [°]	87.336(4)	90
β [°]	79.461(4)	105.772(4)
γ [°]	73.991(4)	90
Volume [Å^3]	1241.4 (4)	921.7(4)
Z	2	2
Density (calculated) [g cm^{-3}]	1.522	1.801
Absorption coefficient [mm^{-1}]	1.137	1.535
F(000)	592	510
Crystal size [mm]	0.28 × 0.14 × 0.12	0.28 × 0.24 × 0.05
Crystal color	blue	blue
Crystal description	rod	plate
θ range of data collection [°]	1.97−28.33	2.17−28.40
Index range	$-9 \le h \le 6$ $-6 \le k \le 14$ $-14 \le l \le 23$	$-12 \le h \le 13$ $-9 \le k \le 9$ $-18 \le l \le 18$
Reflections collected	10779	11593
Independent reflections	4805 [R_{int} = 0.0627]	4565 [R_{int} = 0.0338]
Absorption correction	Siemens SADABS program multi-scan	Bruker AXS Saint program Vers. 6.0
Max./min. transmission	1.00/0.69	−/−
Refinement method	full-matrix least-squares on F^2	full-matrix least-squares on F^2
Data/restraints/parameters	2970/0/364	3533/1/263
Goodness-of-fit on F^2	0.933	0.985
Final *R* indices [$I > 2\sigma(I)$]	*R*1 = 0.0571, *wR*2 = 0.1332	*R*1 = 0.0606, *wR*2 = 0.1574
R indices (all data)	*R*1 = 0.0928, *wR*2 = 0.1515	*R*1 = 0.0774, *wR*2 = 0.1770
Largest diff. peak/hole [e·Å^{-3}]	0.811/−0.440	0.993/−0.577

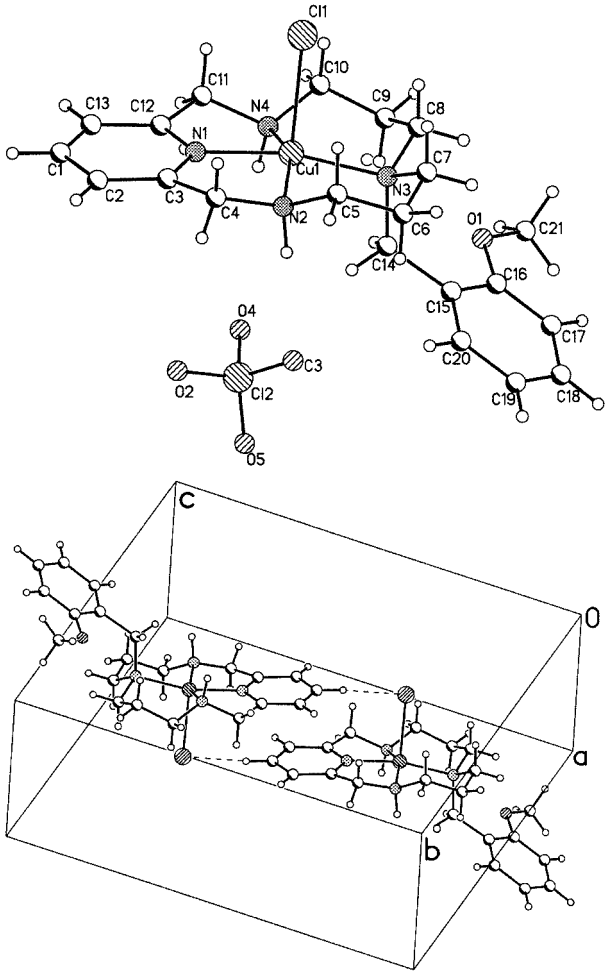

Figure 1. Molecular structure of **Cu-3** in the crystal; selected bond lengths [Å] and angles [°]: Cu1−Cl1 2.564, Cu1−N1 1.938, Cu1−N2 2.023, Cu1−N3 2.026, Cu1−N4 2.054; N1−Cu1−Cl1 92.8, N2−Cu1−Cl1 100.8, N3−Cu1−Cl1 101.1, N4−Cu1−Cl1 97.4, N2−Cu1−N1 81.9, N3−Cu1−N1 166.1, N4−Cu1−N1 81.0, N3−Cu1−N2 95.6, N4−Cu1−N2 155.6, N4−Cu1−N3 96.7

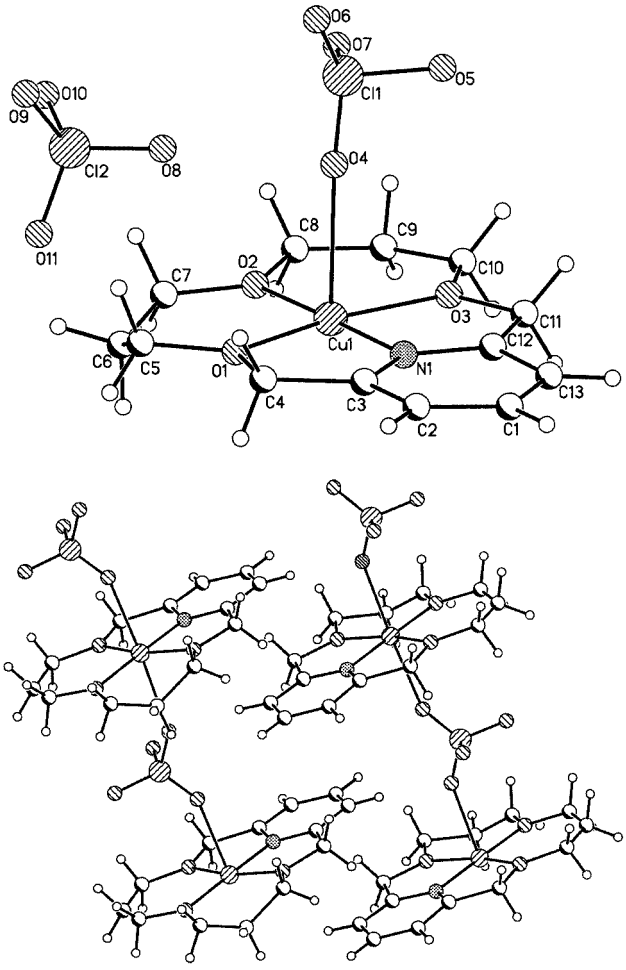

Figure 2. Molecular structure of **Cu-6** in the crystal; selected bond lengths [Å] and angles [°]: Cu1−N1 1.885, Cu1−O1 1.955, Cu1−O2 1.931, Cu1−O3 1.964, Cu1−O4 2.425; O1−Cu1−N1 81.5, O2−Cu1−N1 178.7, O3−Cu1−N1 81.6, O4−Cu1−N1 89.6, O2−Cu1−O1 98.1, O3−Cu1−O1 163.0, O4−Cu1−O1 91.9, O3−Cu1−O2 98.8, O4−Cu1−O2 91.6, O4−Cu1−O3 86.9

coordinated to two Cu^{II} centers as a bridging ligand with Cu^{II}−O distances of 2.425 and 2.433 Å, respectively, in a range (2.2−2.9 Å) commonly observed for axial Cu−O bond lengths.[17] Thus, the coordination geometry of **Cu-6** is essentially tetragonal-octahedral. Oxygen atom O(5) is disordered over two sites with occupancies of 0.68−0.32. In both complexes, the pyridine ring adopts an offset face-to-face orientation.

Infrared Spectra

The spectra of the free ligands **1**−**5** show sharp, medium-intensity bands at 3250−3300 cm^{-1} for the N−H valence vibrations. All ligands showed two bands around 1590 cm^{-1} for the C=N valence vibration of the pyridine ring (Table 2). On Cu^{II} complexation, the N−H valence bands are shifted by about 15−150 cm^{-1} to lower frequencies. For **Cu-1** and **Cu-2** two N−H valence vibrations are observed,

Table 2. Characteristic infrared frequencies [cm^{-1}] of complexes **Cu-1**−**Cu-6**; frequencies of the free ligands **1**−**6** are given in parentheses; the most intense lines are in italics

Complex	$\tilde{\nu}$(N−H)	$\tilde{\nu}$(C=N)	$\tilde{\nu}$(ClO_4^-)
Cu-1	3250, 3221 (3242, 3220)	1609, 1583 (1588, 1576)	1098, 1068, 624
Cu-2	3240, 3223 (3247, 3218)	1605, 1582 (1589, 1571)	1122, 1064, 624
Cu-3	3225, 3163 (3378)	1600, 1583 (1598, 1560)	*1107*, 1054, 623
Cu-4	3243 (3310)	1608, 1585 (1593, 1576)	*1108*, 1066,[a] 624
Cu-5	3354 (3369, 3288)	1607, 1585 (1594, 1578)	1147, 1111, *1091*,[a] 627
Cu-6	– –	1608, 1585 (1590, 1574)	*1085*, 1061, 1038,[a] 621

[a] Assignment ambiguous due to superposition with $\tilde{\nu}$(C−O).

in line with the different chemical environment of the NH groups located in *cis* and *trans* positions with respect to the pyridine nitrogen atom. As the higher wavenumber vibration is missing in the spectra of **Cu-3** and **Cu-4** but found in **Cu-5** (for which the lower wavenumber is absent), we assign this band to the *trans*-oriented NH group. In the complexes, the pyridine ν(C=N) bands are uniformly shifted to higher frequencies by 10−20 cm^{-1}, but virtually unaffected by the variation of the coordinating ring atoms.

The typical ν_3 (antisymmetric stretch) and ν_4 (antisymmetric bent) modes of noncoordinated perchlorate give rise to single, strong absorptions. In complexes **Cu-1**−**Cu-6** the perchlorate absorption at about 1100 cm^{-1} (ν_3) is split into two or three components, whereas the sharp strong band at 620 cm^{-1} (ν_4) remained a singlet. Thus, in the solid state, the symmetry of the perchlorate ions in these complexes is lowered.[7] However, it is not certain whether this is the result of coordination or of crystal packing effects. The latter appears to be more likely because the X-ray structure of **Cu-3** revealed that here the perchlorate is not coordinated to Cu^{II}.

Electronic Absorption

Complexes **Cu-1**−**Cu-6** show broad electronic absorptions in the 550−800-nm region (Table 3), typical for d−d transitions of Cu^{II} in a weak tetragonal field.[24] The absorption maxima show a red-shift (i.e. decreasing ligand-field strength) with increasing number of coordinating oxygen atoms, ranging from λ_{max} = 560 nm for the tetra-*N*-substituted complexes **Cu-1**−**Cu-3** to 793 nm for the tris-O complex **Cu-6**. This red-shift is accompanied by a similar decrease of the molar extinction coefficient ε. With respect to the parent complex **Cu-1**, the methyl and methoxybenzyl substituents in **Cu-2** and **Cu-3**, respectively, have virtually no effect on the absorption maxima but appear to decrease slightly the molar extinction. However, the red-shift of the absorption maxima is markedly different for the various positions with respect to the pyridine ring. Replacement of the nitrogen atom *trans* to the pyridine ring by an oxygen atom, viz. **Cu-1**−**Cu-3** → **Cu-4** and **Cu-5** → **Cu-6**, shifts the absorption maximum by $\Delta\lambda \approx 40$ nm^{-1} toward longer wavelengths, whereas replacement of the *cis* nitrogen atoms, viz. **Cu-1**−**Cu-3** → **Cu-5** and **Cu-4** → **Cu-6**, induces an approximate fivefold stronger shift of $\Delta\lambda \approx 190-200$ nm^{-1}. This discontinuity in the λ_{max} values on *cis*-N→O replacement is paralleled by a decrease of the extinction coefficient ε and a "jump" in the *g* values of the EPR spectra (see below), both indicating a significant change of the coordination geometry from a distorted tetragonal (square-based pyramidal) to a more octahedral tetragonal structure. In line with the stronger effect exerted by a *cis*-oxygen atom, the Cu^{II}-EDTA complex, having a *cis*-2N-2O coordination arrangement, shows a λ_{max} value of ca. 730 nm.[19] For the observed dependencies of the d−d transitions on the ligand substitution pattern, possible Cu^{II} complexes of the hitherto unknown ligands **7** and **8** should have absorption maxima around 700 and 740 nm, respectively.

Table 3. Visible electronic absorptions of Cu^{II} complexes in aqueous solution (298 K)

Complex	λ_{max} [nm]	lgε [$M^{-1}cm^{-1}$]
Cu-1	565[a]	2.56
Cu-2	560[b]	2.29
Cu-3	563	2.13
Cu-4	603	2.18
Cu-5	757	1.42
Cu-6	793	1.36
Cu-EDTA[19]	730	
$Cu(ClO_4)_2$	820	1.04
Cu_2Zn_2SOD[20]	680	2.1

[a] Ref.[21] 544 (2.24) nm, in nitromethane. [b] Ref.[7] 560 (2.25) nm, in methanol; ref.[8] 560 (1.87) nm, in 0.1 M $NaNO_3$.

Electron Paramagnetic Resonance

To check whether the characteristics of the X-ray structures, the UV/Vis spectra, and/or the SOD-like activities (see below) of our Cu complexes are reflected by their EPR spectral features, the EPR spectra of **Cu-1**−**Cu-6** were examined in liquid (Figure 3, Table 4) and frozen (77 K) aque-

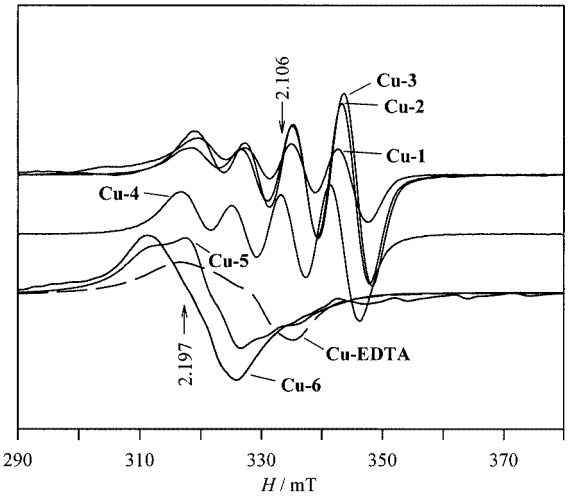

Figure 3. EPR spectra of the copper complexes **Cu-1**−**Cu-6** in aqueous solution (298 K)

Table 4. EPR parameters of Cu^{II} complexes in aqueous solution (298 K)

Complex[a]	g_{app}	A_{iso} [mT]
Cu-1	2.101	7.80
Cu-2	2.099	8.05
Cu-3	2.102	8.32
Cu-4	2.112	8.18
Cu-5	2.176	ca. 4.9
Cu-6	2.197	n.r.[b]
Cu-EDTA	2.134	n.r.

[a] Instrument settings: scan range 150 mT, modulation amplitude 0.5 mT, modulation frequency 100 kHz, microwave power 20 mW, microwave frequency 9.77−9.79 GHz. [b] Not resolved.

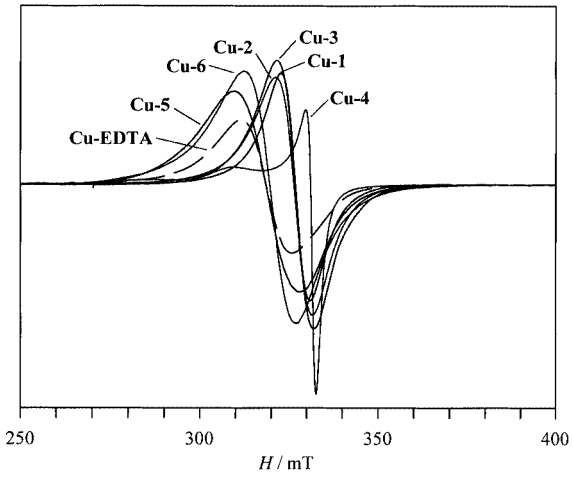

Figure 4. EPR spectra of the copper complexes **Cu-1**−**Cu-6** in frozen aqueous solution (77 K)

Table 5. EPR parameters of Cu complexes in frozen aqueous solution (77 K)

Complex[a]	g_{app}	$g_\perp$	$g_\parallel$	$A_\parallel$ [mT]
Cu-1	2.090	2.086[b]	2.107	≤ 5.5
Cu-2	2.085	2.084[c]	2.105	≤ 5.5
Cu-3	2.082	2.082	2.200	17.4
Cu-4	–	2.056	2.209	≤ 1.5
Cu-5	2.139	–	–	–
Cu-6	2.134	2.128	2.180	8.4
Cu-EDTA	2.136	–	–	–
Cu_2Zn_2SOD[24]	–	2.073	2.267	13.3

[a] Instrument settings: scan range 150 mT, modulation amplitude 0.5 mT, modulation frequency 100 kHz, microwave power 20 mW, microwave frequency 9.52−9.55 GHz. [b] Ref.[8] $g_1 = 2.040$, $g_2 = 2.110$, $g_3 = 2.178$, $A_1 = 4.8$, $A_2 = 9.8$, $A_3 = 199.3$ cm^{-1}; in 1 M $NaClO_4$. [c] Ref. [7] $g_\perp = 2.052$, $g_\parallel = 2.19$; polycrystalline sample, 298 K.

ous solutions (Figure 4, Table 5). The spectra show the expected characteristics of distorted (axially elongated) tetragonal coordination of Cu^{II} ($S = 1/2$) with $g_\parallel > g_\perp$,[18,22] thus indicating a $d_{x^2-y^2}$ ground state. EPR data for Cu^{II}-EDTA and Cu_2Zn_2-SOD are given for comparison. In liquid solution, **Cu-1**−**Cu-3** show virtually identical, nearly isotropic EPR spectra with a well-resolved $^{63/65}$Cu hyperfine splitting in the range of 8 mT (Figure 3), confirming that the additional ring substituents in **Cu-2** and **Cu-3** have only a marginal effect on the spectral properties, in agreement with the absorption spectral properties.

Replacement of the *trans*-nitrogen atom by an oxygen atom in **Cu-4** yields a similarly resolved spectrum with only the apparent *g* factor slightly shifted to higher values. Replacement of the *cis*-nitrogen atoms by oxygen atoms (**Cu-5**), however, results in both a stronger *g* shift to higher values and an increased anisotropy of the spectra, as well as a reduced copper splitting [$a(^{63/65}Cu) \approx 4.9$ mT]. These effects are further pronounced for **Cu-6**. Thus, a replacement of a *cis*-N by O has a stronger effect on the *g* factor than replacement of the *trans*-N by O. These observations strikingly parallel the above-mentioned shifts of the UV/Vis absorption maxima. In addition, the apparent *g* factor of Cu^{II}-EDTA,[23] which has a 2N-2O coordination pattern similar to the arrangement in the macrocycle **8**, lies in between the *g* factors of **Cu-1**−**Cu-4** and **Cu-5** and **Cu-6**. The small spectral features between 330 and 370 mT in the EPR spectrum of **Cu-6** are probably due to a Cu^{II}-containing impurity. Because these signals could not be diminished by repeated recrystallization, they might belong to a copper complex formed from, and in equilibrium with, **Cu-6** in the aqueous phase. The uncommonly low *g* value of about 1.951 [$a(^{63/65}Cu) \approx 8.9$ mT] of this feature would indicate a d_z^2 ground state ($g_\perp > g_\parallel \approx 2$)[18,22] for this species.

In frozen (77 K) aqueous solution (Figure 4) a $^{63/65}$Cu hyperfine splitting can no longer be resolved in any of the spectra. The spectra of **Cu-1**−**Cu-3**, **Cu-5**, and **Cu-6** all consist of a single, broad line with apparent *g* values as given in Table 5. The spectral resolution could not be improved by tenfold dilution and lower microwave power and modulation settings, in agreement with observations by Costa and Delgado[8] who noted for **Cu-1** and related complexes the loss of resolution in solutions of low ionic strength (Table 5, footnote[b]). The anisotropic parameters (Table 5) were evaluated by spectral simulation and are approximate values because of the low resolution. Nevertheless, they are typical for Cu^{II} in a distorted tetragonal environment. As was observed for liquid aqueous solution, the apparent *g* factors are shifted to higher values, from 2.085 to about 2.140, with increasing number of oxygen atoms in the macrocyclic ring. However, two distinct differences compared with the liquid-phase spectra are apparent. First, the spectra of **Cu-5** and **Cu-6** now show approximately the same apparent *g* factor (ca. 2.134−9), similar to that of Cu-EDTA; second, the spectrum of **Cu-4** displays a clear separation of the parallel and perpendicular components of the *g* tensor and also has a smaller linewidth than the other spectra. We have no straightforward explanation for this unique feature of **Cu-4**. As the spectrum of **Cu-4** is strikingly similar to those observed for polycrystalline samples of **Cu-2** and related complexes at ambient temperature,[4] it might indicate that the coordination sphere in frozen water is very similar to that in the solid state.

Electrochemical Properties

Cyclic voltammograms of complexes **Cu-1**−**Cu-4** and **Cu-6** were examined in oxygen-free aqueous solution at room temperature. Potassium chloride was employed as supporting electrolyte to achieve a better correspondence with the conditions of the SOD activity measurements (see below). All complexes showed a quasi-reversible redox wave (E^1) in the range +0.37 to +0.42 V vs. NHE and an apparent irreversible cathodic peak (E^2_{pc}) between −0.13 and −0.36 V (Table 6). The latter potential might be quasi-reversible but the corresponding anodic peak was overlayed by a strong adsorption peak which appeared between 0 and +0.15 V on the subsequent oxidation cycle. Very similar voltammograms were obtained for hydrated Cu^{II} ions from solutions of copper(II) perchlorate and copper(II) sulfate un-

der the same conditions. The data of Table 6 display no dramatic variation of the potentials with the nature of the ligands. The quasi-reversible potentials $E^1_{1/2}$ of **Cu-1**−**Cu-3** differ only by 10 mV, the cathodic peak potentials E^2_{pc} by ca. 50 mV. Replacement of N by O in the macrocyclic ligand (**Cu-4**, **Cu-6**) shifted the E^1 potentials toward slightly (20−40 mV) more positive values, approaching the values for $CuSO_4$ and $Cu(ClO_4)_2$. The same is true for E^2_{pc} with the exception of **Cu-4** for which a cathodic shift of ca. 200 mV was observed. However, inspection of Table 6 clearly reveals that neither the E^1 nor the E^2_{pc} potential would account for the unique, though low SOD activity of **Cu-3** (see below, Table 7), as its anodic redox potential does not differ from those of **Cu-1** and **Cu-2**, and, also, the SOD activities of all copper compounds (see below) do not parallel the variation of the E^2_{pc} values. Thus, the redox potentials of the Cu^{II} complexes are not essentially associated with their SOD activities.

Table 6. Cyclic voltammetric data [V vs. NHE] of the copper(II) complexes

Compound[a]	E^1_{pa}	E^1_{pc}	$E^1_{1/2}$[b]	E^2_{pc}[c]
Cu-1	0.439	0.322	0.381	−0.164
Cu-2	0.438	0.317	0.378	−0.138
Cu-3	0.465	0.287	0.376	−0.214
Cu-4	0.491	0.318	0.405	−0.358
Cu-6	0.466	0.366	0.416	−0.056
$Cu(ClO_4)_2$	0.463	0.335	0.400	−0.068
$CuSO_4$	0.446	0.314	0.414	−0.005

[a] At 1 mM and a scan rate of 0.1 V s^{-1}. [b] Quasi-reversible, $E_{1/2} = (E_{pa} + E_{pc})/2$. [c] Irreversible or quasi-reversible.

Superoxide Dismutase Activity

Copper(II) complexes **Cu-2**−**Cu-4**, and **Cu-6** were examined with regard to their Superoxide Dismutase (SOD) mimetic activity by the method of Paoletti et al.[25] For comparison purposes, hydrated Cu^{II} [employed as $Cu(ClO_4)_2$] was also investigated. The applied method is based on the oxidation of β-nicotinamide adenine dinucleotide (β-NADH) by mercaptoethanol/EDTA/Mn^{2+} at pH = 7.4. In the presence of molecular oxygen, this system generates superoxide ($O_2^{\cdot -}$), which, in turn, oxidizes NADH to NAD^+. Based on the kinetics of the oxidation of NADH in the presence and absence (control) of copper(II) complexes, the SOD-mimetic potential was determined. Addition of SOD or a SOD-active compound inhibits the oxidation of NADH, which is monitored UV-spectroscopically by the retarded decay of the absorption of NADH at 340 nm. After an initially progressive course, the decline of the absorption follows apparent zero-order kinetics (Figure 5, inset). These parts of the decay traces were used for the subsequent evaluation of the rates. To determine the SOD activity, the percentage of the rate of inhibition of NADH oxidation (control: absence of SOD-mimic = 100%) was plotted against the initial concentration of the copper complexes (Figure 5). For all complexes the inhibition of the oxidation rate is not proportional to the concentrations of copper complexes but rather follows an exponential dependence. The IC_{50} value, that is the amount of complex reducing the rate of the NADH oxidation by 50%, was extracted from the graphs (Table 7). Since catalase does not interfere in the above reaction, this enzyme was used to remove the produced hydrogen peroxide so as to determine whether the peroxide and/or its possible reaction products affect the assay. As the catalytic activity in the presence of catalase[26] did not change, inhibition by hydrogen peroxide and its possible products can be excluded.

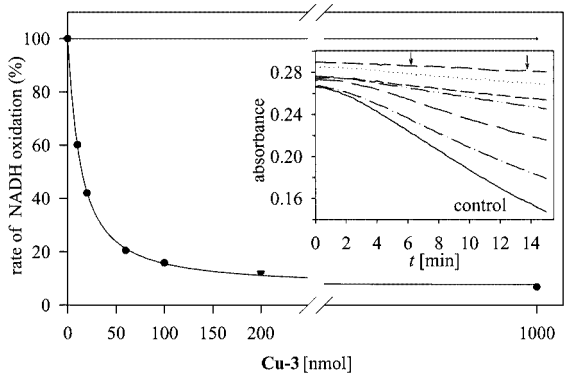

Figure 5. Inhibition of NADH oxidation as a function of **Cu-3** concentration; inset: kinetic traces of NADH oxidation monitored at 340 nm at different concentrations of **Cu-3**

Table 7. Comparison of superoxide dismutase activity at 296 K

Compound	IC_{50} [μM]	Cu/NADH ratio
Cu-2	247	1:1.07
Cu-3	28	1:9.46
Cu-4	206	1:1.29
Cu-6	126	1:2.10
$Cu(ClO_4)_2$	247	1:1.07

The IC_{50} values and the Cu/NADH ratios listed in Table 7 reveal that complexes **Cu-2** and **Cu-4** do not show any true catalytic activity, rather, they convert $O_2^{\cdot -}$ in a roughly 1:1 stoichiometric ratio, similar to copper(II) perchlorate. Likewise, **Cu-6** does not appear to be a catalyst, reacting with $O_2^{\cdot -}$ in a 1:2 stoichiometry. Hence, simple exchange of the coordinating atoms, i.e. N vs. O, in the macrocyclic ring does not effect the SOD-like activity of this type of Cu^{II} complexes. However, for complex **Cu-3**, which carries a methoxybenzyl pendent arm, a low but unequivocal catalytic activity is found. The data indicate a turnover of about 10, i.e. one molecule of the complex decomposes about ten molecules of superoxide before being deactivated.

Investigation of the SOD-mimetic activity of complexes by employing indirect methods like the one chosen here are frequently hampered because "free" (hydrated) Cu^{II} ions also react with $O_2^{\cdot -}$, as is demonstrated here by $Cu(ClO_4)_2$. Thus, the question arises as to whether the present copper complexes or low amounts of free Cu^{II} ions, deriving from dissociation of the complexes or impurities, are responsible for the observed reaction. The latter possibility can be ex-

cluded on the basis of the control experiments with copper(II) perchlorate. Further, the stability of our complexes was confirmed by EPR experiments in which a tenfold excess of EDTA added to aqueous solutions of the complexes produced no detectable changes in the EPR spectra of **Cu-1**−**Cu-6**.

The catalytic activity of **Cu-3** is rather surprising as the above spectroscopic and electrochemical data do not indicate any unique physicochemical properties in solution compared with the analogues **Cu-1** and **Cu-2**. Indeed, the oxygen-substituted systems **Cu-4**−**Cu-6** which indeed show marked variations in their UV/Vis and EPR spectra, behave very similarly to **Cu-1** and **Cu-2**. Exploratory experiments were performed with regard to the mechanistic background for the enhanced activity of **Cu-3**. In complex **Cu-3**, the fifth coordination site in the solid state is occupied by a chloride ion, whereas in the nonactive complexes **Cu-2**, **Cu-4**, and **Cu-6** this site is occupied by a second perchlorate ion. Thus, the chloride coordination might be responsible for the catalytic activity of **Cu-3**. Experiments were, therefore, performed in which large amounts (50 mM) of potassium chloride were added to the reaction mixture. However, no changes in the catalytic activities of all complexes were detected. As neither contamination by "free" Cu^{II} nor different coordinating counterions account for the different activity of **Cu-3**, it appears that the methoxybenzyl side chain in **Cu-3** is responsible. The X-ray structure of **Cu-3** showed that the methoxybenzyl substituent is not coordinated via the oxygen atom to the copper center but rather directed outward (Figure 3). Such an arrangement would make a significant influence of the pendent arm on the SOD activity very unlikely. However, in solution the situation might change due to free rotational movement of the methoxybenzyl group. Trial PM3(tm) calculations indeed favor (at least in the gas phase) an arrangement of the substituent where the methoxy oxygen atom is coordinated to the central Cu^{II} ion (Figure 6).

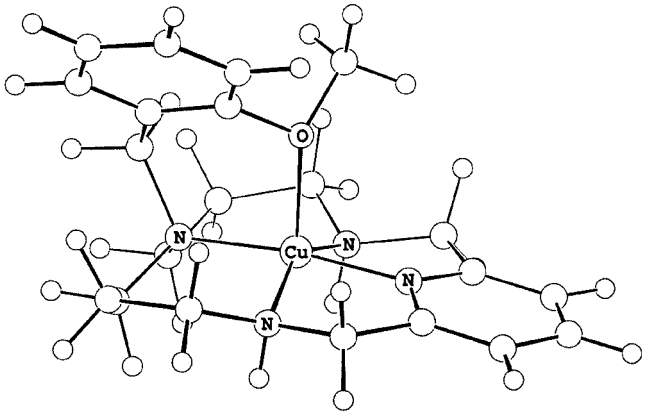

Figure 6. Optimized PM3 structure for **Cu-3**

Therefore, in aqueous solution the methoxybenzyl substituent might "protect" one of the axial positions against further, deactivating reactions (e.g. from attack of a second superoxide molecule) when the substrate superoxide has associated to the opposite side. Such a blocking function might be a crucial feature for the catalytic activity of the complex. However, from the currently available data, no further conclusions concerning the reaction mechanism can be made. Further work is necessary for a deeper insight into the mechanism of superoxide dismutation.

Experimental Section

Instrumentation: ^1H and ^{13}C NMR spectra: Bruker DRX 500 and Varian Gemini 200. Melting points (uncorrected): Elektrothermal 9100. IR: Bio-Rad Series FTS 135 FT-IR. UV/Vis: J&M TIDAS Detector NMC 301. EPR: Bruker ESP 300E. Elemental analysis: Carlo Erba 1010 CHNSO. Cyclic voltammetry: ECO-Chemie Autolab GPES.

Materials: The following compounds were prepared according to published procedures: pyridine-2,6-dicarbaldehyde,[27] 3,7,11,17-teraazabicyclo[11.3.1]heptadeca-1(17),13,15-triene (**1**),[6] {2,12-dimethyl-3,7,11,17-tetraazabicyclo[11.3.1]heptadeca-1(17),2,11,13,15-pentaene}nickel(II) perchlorate,[13] {2,12-dimethyl-3,7,11,17-tetraazabicyclo[11.3.1]heptadeca-1(17),13,15-triene}nickel(II) perchlorate,[13] (2*R*,12*S*)-2,12-dimethyl-3,7,11,17-tetraazabicyclo[11.3.1]-heptadeca-1(17),13,15-triene monohydrate (**2**),[28,29] *N*,*N*-bis(2-cyanoethyl)-2-methoxybenzylamine, *N*,*N*-bis(3-aminopropyl)-2-methoxybenzylamine,[1] 7-(2-methoxybenzyl)-3,7,11,17-tetraazabicyclo[11.3.1]heptadeca-1(17),13,15-triene (**3**),[1] 2,6-bis[(tosyloxy)methyl]pyridine,[30] dipropanolamine,[31] 4-oxa-1,7-heptanediol,[14] 4-oxaheptane-1,7-diyl ditosylate,[14] 3,7,11-trioxa-17-azabicyclo[11.3.1]heptadeca-1(17),13,15-triene (**6**).[14] Reduced adenine dinucleotide (β-NADH, disodium salt) and diethyleneaminotetraacetic acid (EDTA) were obtained from Sigma, while manganese(II) chloride dihydrate and 2-mercaptoethanol were supplied by Merck and 3,3′-oxydipropionitrile by Fluka. Reagents and solutions: triethanolamine/diethanolamine (Tea-Dea) buffer (100 mM each, pH = 7.4); NADH (7.5 mM); EDTA/$MnCl_2$ (100 mM/50 mM); mercaptoethanol (10 mM).

3,3′-Oxydipropaneamine: The literature synthesis[32] was improved as follows: Raney nickel (3 g) was added to a solution of 3,3′-oxydipropionitrile (2.06 g, 16.6 mmol), dissolved in methanol (40 mL), containing anhydrous ammonia (5.2 g, 0.31 mol). The nitrile was hydrogenated under pressure (8 bar) at room temperature, until no drop in pressure was observed (10 h). The residue was filtered off and the product obtained by distillation under reduced pressure (2.0 g, 15.1 mmol, 91%). ^1H NMR (500 MHz, CD_3OD): δ = 1.66 (m, 4 H, 2 × CH_2), 2.66 (t, ^3J = 6.5 Hz, 4 H, 2 × CH_2), 3.44 (t, ^3J = 6.2 Hz, 4 H, 2 × CH_2) ppm. ^{13}C NMR (75 MHz, CD_3OD): δ = 33.77 (2 × CH_2), 40.11 (2 × CH_2), 70.13 (2 × CH_2) ppm.

7-Oxa-3,11,17-triazabicyclo[11.3.1]heptadeca-1(17),13,15-triene (4): A solution of pyridine-2,6-dicarbaldehyde (3.25 g, 24.0 mmol) in ethanol was added to a stirred solution of copper nitrate trihydrate (5.80 g, 24.0 mmol) in water (65 mL), resulting in a pale green mixture. A solution of 3,3′-oxydipropioamine (3.24 g, 24.5 mmol) in ethanol (10.0 mL) was then added dropwise with rapid stirring over 30 min and the resulting dark blue solution was refluxed for 2 h, then cooled to 5 °C in an ice/brine bath and sodium borohydride (2.30 g, 60.4 mmol) added. After 30 min, the solution was stirred at room temperature for 2 h, heated at 60 °C for 1 h, and stirred further at room temperature for several hours. The copper(II) was removed by treating the mixture with sodium sulfide nonahydrate (14.41 g, 60 mmol) followed by stirring at 60 °C for 1 h, and the solution was then cooled and the copper(II) sulfide removed by

filtration through Celite. Ethanol was evaporated, the residue extracted three times with dichloromethane, and the combined extracts dried with $MgSO_4$. After removal of the dichloromethane by evaporation, the resultant light brown residue was purified by chromatography (chloroform, neutral aluminium oxide). The product was obtained as a colourless solid (3.16 g, 13.4 mmol, 56%). ^{1}H NMR (500 MHz, $CDCl_3$): δ = 1.82 (m, 4 H, CH_2), 2.59 (t, ^3J = 5.5 Hz, 4 H, CH_2), 3.54 (t, ^3J = 5.5 Hz, 4 H, CH_2), 3.70 (s, 2 H, N*H*), 3.89 (s, 4 H, CH_2), 6.99 (d, ^3J = 7.6 Hz, 2 H, C*H*), 7.52 (dd, 1 H, ^3J = 7.6 Hz, C*H*) ppm. ^{13}C NMR (75 MHz, $CDCl_3$): δ = 29.28 (*C*H$_2$), 45.39 (*C*H$_2$), 53.91 (*C*H$_2$), 68.34 (*C*H$_2$), 120.81 (*C*H), 136.72 (*C*H), 158.53 (*C*) ppm. $C_{13}H_{21}N_3O$ (235.33): calcd. C 66.35, H 8.99, N 17.86; found C 66.05, H 9.17, N 17.61.

3,11-Dioxa-7,17-diazabicyclo[11.3.1]heptadeca-1(17),13,15-triene (5): Macrocycle **5** was prepared from (1.81 g, 4.0 mmol) 2,6-bis[(tosyloxy)methyl]pyridine and dipropanolamine (0.54 mg, 4.0 mmol) in a similar fashion to the procedure of Bradshaw et al.[14] The product thus obtained was a colourless solid (0.51 g, 2.16 mmol, 54%). ^{1}H NMR (200 MHz, $CDCl_3$): δ = 1.91 (m, 4 H, CH_2), 3.05 (br. m, 8 H, CH_2), 4.67 (s, 4 H, CH_2), 7.20 (d, 2 H, C*H*), 7.68 (dd, 1 H, C*H*) ppm. ^{13}C NMR (50 MHz, $CDCl_3$): δ = 30.12 (*C*H$_2$), 49.15 (*C*H$_2$), 65.83 (*C*H$_2$), 72.72 (*C*H$_2$), 117.12 (*C*H), 123.52 (*C*H), 158.88 (*C*) ppm. $C_{13}H_{20}N_2O_2$ (236.31): calcd. C 66.07, H 8.53, N 11.86; found C 66.33, H 8.55, N 11.92.

Copper Complexes Cu-1−Cu-6: The preparation of **Cu-1**[6] and **Cu-2**[7] has been reported before. All solid complexes were obtained in good yields (> 65%) by mixing ethanolic solutions of the appropriate ligands with equimolar solutions of cupric perchlorate hexahydrate in ethanol at room temperature. The precipitated complexes were isolated by filtration and purified by washing several times with cold ethanol. Whereas complexes **Cu-1**, **Cu-2**, and **Cu-4−Cu-6** were instantaneously formed on mixing of the reactants, addition of an equimolar amount of copper(II) perchlorate in ethanol to an ethanolic solution of ligand **3** initially led to rapid formation of a yellow precipitate which according to elemental analysis and EPR spectroscopy represented a Cu^{II}−ligand complex of 1:2 stoichiometry, $[Cu^{II}(\mathbf{3})_2](ClO_4)_2$ (60% yield relative to **3**). When the reaction mixture without prior separation of this complex was allowed to stand for 12 h at ambient temperature, violet crystals of complex **Cu-3** were obtained in 68% yield.

CAUTION: Metal perchlorate salts containing organic ligands are potentially explosive, and should be handled with care!

Characterization of Complexes Cu-1−Cu-6

Cu-1: Blue-purple powder (0.39 g, 68%). IR (KBr): $\tilde{\nu}$ = 3242 (NH), 3084 (CH_{Ph}), 2936 (CH_{aliph}), 624 (ClO_4) cm^{-1}. $C_{13}H_{22}Cl_2CuN_4O_8$ (496.80): calcd. C 31.43, H 4.46, Cu 12.79, N 11.28; found C 31.14, H 4.41, Cu 12.58, N 10.99. UV (water): λ_{max} (lg ε) = 565 (2.56) nm.

Cu-2: Violet-blue powder (0.76 g, 76%), decomp. 254 °C. IR (KBr): $\tilde{\nu}$ = 3223 (NH), 3094 (CH_{Ph}), 2943 (CH_{aliph}), 624 (ClO_4) cm^{-1}. $C_{15}H_{26}Cl_2CuN_4O_8$ (524.86): calcd. C 34.33, H 4.99, Cu 12.11, N 10.68; found C 34.29, H 4.97, Cu 11.84, N 10.39. UV (water): λ_{max} (lg ε) = 254 (3.90), 560 (2.29) nm.

Cu-3: Violet-blue crystals (0.39 g, 68%), decomp. 231 °C. IR (KBr): $\tilde{\nu}$ = 3226 (NH), 3068 (CH_{Ph}), 2934 (CH_{aliph}), 2893 ($CH_{methyl\ ether}$), 1600 (NH), 1248 ($CO_{aryl\ alkyl\ ether}$), 622 (ClO_4) cm^{-1}. $C_{21}H_{30}Cl_2CuN_4O_5$ (553.73): calcd. C 45.61, H 5.47, Cu 11.49, N 10.13; found C 45.31, H 5.55, Cu 11.41, N 9.84. FAB (glycerol): *m/z* (%) = 516 (3), 417 (15), 355 (34). UV (water): λ_{max} (lg ε) = 256 (3.89), 563 (2.13) nm.

Cu-4: Blue crystals (0.83 g, 73%), decomp. 290 °C. IR (KBr): $\tilde{\nu}$ = 3242 (NH), 3092 (CH_{Ph}), 2951 (CH_{aliph}), 1608 (NH), 1108 (COC), 624 (ClO_4) cm^{-1}. $C_{13}H_{21}Cl_2CuN_3O_9$ (497.78): calcd. C 31.37, H 4.25, Cu 12.77, N 8.44; found C 31.72, H 4.26, Cu 12.66, N 8.52. FAB (glycerol): *m/z* (%) = 397 (22), 298 (30). UV (water): λ_{max} (lg ε) = 255 (3.82), 603 (2.15) nm.

Cu-5: Light blue crystals (0.24 g, 65%), decomp. 291 °C. IR (KBr): $\tilde{\nu}$ = 3078 (CH_{Ph}), 2957 (CH_{aliph}), 1605 (NH), 627 (ClO_4) cm^{-1}. $C_{13}H_{20}Cl_2CuN_2O_{10}$ (498.76): calcd. C 31.31, H 4.04, Cu 12.74, N 5.62; found C 30.98, H 3.94, Cu 12.89, N 5.47. UV (water): λ_{max} (lg ε) = 757 (1.42) nm.

Cu-6: Turquoise crystals (0.36 g, 72%), decomp. 292 °C. IR (KBr): $\tilde{\nu}$ = 3084 (CH_{Ph}), 2957 (CH_{aliph}), 621 (ClO_4) cm^{-1}. $C_{13}H_{19}Cl_2CuNO_{11}$ (499.73): calcd. C 31.24, H 3.83, Cu 12.72, N 2.80; found C 31.52, H 3.82, Cu 12.43, N 2.99. FAB (glycerol): *m/z* (%) = 300 (100), 238 (83). UV (water): λ_{max} (lg ε) = 264 (3.59), 793 (1.36) nm.

Aqueous solutions of the complexes all had pH values between 7 and 8.

Kinetic Measurements: The principle of the method is based on the oxidation of NADH, mediated by superoxide radical, in a purely chemical system developed by Paoletti et al.[25] To monitor the assay we added the following solutions (see materials) into a cuvette (1-mm cell): 400 μL Tea-Dea buffer (100 mM each), 20 μL NADH solution (7.5 mM), 12.5 μL EDTA/$MnCl_2$ solution (100 mM/50 mM) and 50 μL of sample or buffer were mixed thoroughly. In a second series of experiments the reaction mixture was supplemented with 50 mM KCl. The reaction was started by rapid mixing with 50 μL of mercaptoethanol (10 mM). Rates of NADH oxidation, observed at 340 nm, were initially low, then increased progressively to yield good linear kinetics and an 8-min window was used for our calculations. The maximal rates obtained are expressed as a percentage of the control and plotted against the complex concentracion. One unit of the SOD-mimic is the amount of copper complex capable of inhibiting by 50% the rate of NADH oxidation observed in the control.

EPR Spectroscopy: X-band (9.5 GHz) EPR spectra were recorded from 1−3 mM solutions of the complexes in oxygen-free, deionized water in a TM_{110} wide-bore cavity (Bruker). For liquid solutions, a 0.4 mm inner diameter quartz flat cell (Wilmad) was used; measurements at 77 K were performed in 4 mm Suprasil quartz tubes immersed in a liquid nitrogen dewar insert. Spectral simulations were carried out with the Simfonia program (Bruker). The concentration of the copper complexes in liquid and frozen solution was checked by numerical double integration (WinEPR software, Bruker) of the EPR spectra and comparison with the integrated EPR signal of a 1 mM Cu^{II}-EDTA solution. In all cases the integration accounted for > 90% purity of the complexes.

Cyclic Voltammetry: Cyclic voltammetric measurements were performed at 20 °C in aqueous solution under nitrogen. Complex concentrations of 1 mM were employed, and 100 mM KCl was used as supporting electrolyte. A 3 mm diameter glassy-carbon working electrode, an Ag/AgCl reference electrode, and a Pt-wire counter electrode were used. Scan rates were varied from 0.01 to 1.0 V s^{-1}. Electrochemical potentials were converted into the normal hydrogen electrode (NHE) scale by addition of 0.222 V.

X-ray Crystallographic Study: CCDC-188550 (**Cu-3**) and -188551 (**Cu-6**) contain the supplementary crystallographic data for this paper. These data can be obtained free of charge at

www.ccdc.cam.ac.uk/conts/retrieving.html [or from the Cambridge Crystallographic Data Centre, 12 Union Road, Cambridge CB2 1EZ, UK; Fax: (internat.) + 44-1223/336-033; E-mail: deposit@ccdc.cam.ac.uk].

Acknowledgments

This work was supported by the Deutsche Forschungsgemeinschaft (SFB, 452).

[1] S. Autzen, H.-G. Korth, H. de Groot, R. Sustmann, *Eur. J. Org. Chem.* **2001**, 3119−3125.
[2] B. Halliwell, *New Phytol.* **1974**, *73*, 1075−1086.
[3] T. Nagano, *Yuki Gosei Kagaku* **1989**, *47*, 843−854. K. Jitsukawa, M. Harata, H. Arii, H. Sakurai, H. Masuda, *Inorg. Chim. Acta* **2001**, *324*, 108−116.
[4] J. R. Sorenson, *Prog. Med. Chem.* **1989**, *26*, 437−568.
[5] D. P. Riley, *Chem. Rev.* **1999**, *99*, 2573−2587.
[6] K. P. Balakrishnan, H. A. A. Omar, P. Moore, N. W. Alcock, G. A. Pike, *J. Chem. Soc., Dalton Trans.* **1990**, 2965−2969.
[7] L. F. Lindoy, N. E. Tokel, L. B. Anderson, D. H. Busch, *J. Coord. Chem.* **1971**, *1*, 7−16.
[8] J. Costa, R. Delgado, *Inorg. Chem.* **1993**, *32*, 5257−5265.
[9] V. Felix, M. J. Calhorda, J. Costa, R. Delgado, C. Brito, M. T. Duarte, T. Arcos, M. G. B. Drew, *J. Chem. Soc., Dalton Trans.* **1996**, 4543−4553.
[10] P. Chaudhuri, K. Wieghardt, *Progr. Inorg. Chem.* **2001**, *50*, 151−216.
[11] R. R. Fenton, R. Gauci, P. C. Junk, L. F. Lindoy, R. C. Luckay, G. V. Meehan, J. R. Price, P. Turner, G. Wei, *J. Chem. Soc., Dalton Trans.* **2002**, 2185−2193.
[12] E. V. Rybak- Akimova, A. Y. Nazarenko, S. S. Silchenko, *Inorg. Chem.* **1999**, *38*, 2974−2980. M. Mikuriya, K. Hamada, S. Kida, I. Murase, *Bull. Chem. Soc. Jpn*, **1985**, *58*, 1839−1840. J. Costa, R. Delgado, M. G. B. Drew, V. Felix, *J. Chem. Soc., Dalton Trans.* **1999**, 4331−4339. M. Di Casa, L. Fabbrizzi, M. Licchelli, A. Poggi, D. Sacchi, M. Zema, *J. Chem. Soc., Dalton Trans.* **2001**, 1671−1675. K. Panneerselvam, T.-H. Lu, T.-Y. Chi, F.-L. Liao, C.-S. Chung, *Anal. Sci.,* **2000**, *16*, 441−442. K. Mochizuki, S. Miyashita, *Chem. Lett.* **1996**, 899−900. H. Keypour, S. Salehzadeh, R. G. Pritchard, R. V. Parish, *Inorg. Chem.* **2000**, *39*, 5787−5790.
[13] J. L. Karn, D. H. Busch, *Inorg. Chem.* **1969**, *8*, 1149−1153.
[14] J. S. Bradshaw, J. M. Guynn, S. G. Wood, B. E. Wilson, N. K. Dalley, R. M. Izatt, *J. Heterocycl. Chem.* **1987**, *24*, 415−419.
[15] M. M. Abu-Omar, L. D. McPherson, J. Arias, V. M. Béreau, *Angew. Chem.* **2000**, *112*, 4480−4483; *Angew. Chem. Int. Edit.* **2000**, *39*, 4310−4313.
[16] V. L. Goedken, Y.-A. Park, *J. Chem. Soc., Chem. Commun.* **1975**, 214−215.
[17] T. Murakami, S. Hatakeyama, S. Igarashi, Y. Yukawa, *Inorg. Chim. Acta* **2000**, *310*, 96− 102.
[18] B. J. Hathaway in *Comprehensive Coordination Chemistry*, vol. 5, chapter 53 (Ed.: G. Wilkinson), Pergamon Press, Oxford, **1987**, p. 594−744.
[19] C. K. Jørgensen, *Acta Chem. Scand.* **1955**, *9*, 1362−1377.
[20] M. Linss, U. Weser, *Inorg. Chim. Acta* **1986**, *125*, 117−121.
[21] N. W. Alcock, K. P. Balakrishnan, P. Moore, G. A. Pike, *J. Chem. Soc., Dalton Trans.* **1987**, 889−894.
[22] J. R. Pilbrow *Transition Metal Ion Electron Paramagnetic Resonance*, Clarendon Press, Oxford, **1990**, pp. 9, 30, 154, 484.
[23] F. S. Stephens, *J. Chem. Soc. A* **1969**, 1723−1734.
[24] R. A. Lieberman, R. H. Sands, J. A. Fee, *J. Biol. Chem.* **1982**, *257*, 336−344.
[25] F. Paoletti, D. Aldinucci, A. Mocali, A. Caparrini, *Anal. Biochem.* **1986**, *154*, 536−541.
[26] F. Paoletti, A. Mocali, *Methods Enzymol.* **1990**, *186*, 209−220.
[27] N. W. Alcock, R. G. Kingston, P. Moore, C. Pierpoint, *J. Chem. Soc., Dalton Trans.* **1984**, 1937−1943.
[28] A. C. Melnyk, N. K. Kildahl, A. R. Rendina, D. H. Busch, *J. Am. Chem. Soc.* **1979**, *101*, 3232−3240.
[29] C. J. Cairns, R. A. Heckman, A. C. Melnyk, W. M. Davis, D. H. Busch, *J. Chem. Soc., Dalton Trans.* **1987**, 2505−2510.
[30] J. S. Bradshaw, P. Huszthy, C. W. McDaniel, C. Y. Zhu, N. K. Dalley, R. M. Izatt, *J. Org. Chem.* **1990**, *55*, 3129−3137.
[31] C. Granier, R. Guilard, *Tetrahedron* **1995**, *51*, 1197−1208.
[32] P. F. Wiley, *J. Am. Chem. Soc.* **1946**, *68*, 1867−1868.

Received July 12, 2002
[I02379]